Research Article
Vol. 26, No. 17 | 20 Aug 2018 | OPTICS EXPRESS 22135
Optics EXPRESS

Actively Q-switched tunable narrow bandwidth milli-Joule level Tm:YLF laser

UZZIEL SHEINTOP,[1,2,3] EYTAN PEREZ,[1] DANIEL SEBBAG,[1] PAVEL KOMM,[2] GILAD MARCUS,[2] AND SALMAN NOACH[1,4]

[1] *Department of Applied Physics, Electro-optics Engineering Faculty, Jerusalem College of Technology, Havaad Haleumi 21, Jerusalem, Israel*
[2] *Department of Applied Physics, The Hebrew University of Jerusalem, Jerusalem, Israel*
[3] *uzziel.shaintop@mail.huji.ac.il*
[4] *salman@jct.ac.il*

Abstract: A pulsed high energy and narrow bandwidth tunable Tm:YLF laser at the milli-Joule level is demonstrated. The spectral bandwidth was narrowed down to 0.15 nm FWHM, while 33 nm of tunability range between 1873 nm and 1906 nm was achieved using a pair of YAG Etalons. The laser was actively Q-switched using an acousto-optic modulator and mJ level pulse energy was measured along the whole tuning range at a repetition rate of 1 kHz. Up to 1.97 mJ of energy per pulse was achieved at a pulse duration of 37 ns at a wavelength of 1879 nm, corresponding to a peak-power of 53.2 kW and at a slope efficiency of 36 %. The combination of both high energy pulsed lasing and spectral tunability, while maintaining narrow bandwidth across the whole tunability range, enhances the laser abilities, which could enable new applications in the sensing, medical and material processing fields.

OCIS codes: (140.3600) Lasers, tunable; (140.3580) Lasers, solid-state; (140.3540) Lasers, Q-switched; (140.3070) Infrared and far-infrared lasers.

References and links

1. A. Godard, "Infrared (2-12 μm) solid-state laser sources: a review," Comptes Rendus Physique **8**, 1100–1128 (2007).
2. K. Scholle, P. Fuhrberg, P. Koopmann and S. Lamrini, *2 μm Laser Sources And Their Possible Applications* (INTECH Open Access Publisher, 2010).
3. I. Sorokina and K. Vodopyanov, *Solid-State Mid-Infrared Laser Sources* (Springer, 2003).
4. C. Richter, A. Matic, J. Wells, E. Jansen and J. Walsh, "Neural stimulation with optical radiation," Laser & Photonics Rev. **5**, 68–80 (2010).
5. O. Eremeikin, A. Savikin, K. Pavlenko and V. Sharkov, "Diode-pumped tunable Tm:YLF laser for mid-infrared gas spectroscopy," Quantum Electronics **40**, 471–474 (2010).
6. J. Peltola, M. Vainio, T. Hieta, J. Uotila, S. Sinisalo, M. Metsala, M. Siltanen and L. Halonen, "High sensitivity trace gas detection by cantilever-enhanced photoacoustic spectroscopy using a mid-infrared continuous-wave optical parametric oscillator," Opt. Express **21**, 10240 (2013).
7. P. Komm, U. Sheintop, S. Noach and G. Marcus, "87 fs CEP-stable Cr:ZnSe laser system," Laser Phys. **28**, 025301 (2018).
8. Z. Qin, J. Liu, G. Xie, J. Ma, W. Gao, L. Qian, P. Yuan, X. Xu, J. Xu and D. Zhou, "Spectroscopic characteristics and laser performance of Tm:$CaYAlO_4$ crystal," Laser Phys. **23**, 105806 (2013).
9. N. Coluccelli, G. Galzerano, P. Laporta, F. Cornacchia, D. Parisi and M. Tonelli, "Tm-doped $LiLuF_4$ crystal for efficient laser action in the wavelength range from 1.82 to 2.06 μm," Opt. Lett. **32**, 2040 (2007).
10. M. Sun, J. Long, X. Li, Y. Liu, H. Ma, Y. An, X. Hu, Y. Wang, C. Li and D. Shen, "Widely tunable Tm:LuYAG laser with a volume Bragg grating," Laser Phys. Lett. **9**, 553–556 (2012).
11. L. Wang, C. Gao, M. Gao, L. Liu and F. Yue, "Diode-pumped 2 μm tunable single-frequency Tm:LuAG laser with intracavity etalons," Appl. Opt. **52**, 1272 (2013).
12. T. Feng, S. Zhao, K. Yang, G. Li, D. Li, J. Zhao, W. Qiao, J. Hou, Y. Yang, J. He, L. Zheng, Q. Wang, X. Xu, L. Su and J. Xu, "Diode-pumped continuous wave tunable and graphene Q-switched Tm:LSO lasers," Opt. Express **21**, 24665 (2013).
13. T. Feng, K. Yang, S. Zhao, J. Zhao, W. Qiao, T. Li, L. Zheng and J. Xu, "Broadly wavelength tunable acousto-optically Q-switched Tm:Lu_2SiO_5 laser," Appl. Opt. **53**, 6119 (2014).
14. F. Di Trapani, X. Mateos, V. Petrov, A. Agnesi, U. Griebner, H. Zhang, J. Wang and H. Yu, "Continuous-wave laser performance of Tm:$LuVO_4$ under Ti:sapphire laser pumping," Laser Phys. **24**, 035806 (2014).

#332808 https://doi.org/10.1364/OE.26.022135
Journal © 2018 Received 28 May 2018; revised 18 Jul 2018; accepted 25 Jul 2018; published 13 Aug 2018

15. W. Gao, G. Xie, J. Ma, M. Liu, P. Yuan, L. Qian, H. Yu, H. Zhang, J. Wang and J. Zhang, "Spectroscopic characteristics and efficient laser operation of Tm:CLNGG disordered crystal," Laser Phys. Lett. **10**, 055809 (2013).
16. U. Sheintop, E. Perez and S. Noach, "Watt-level tunable narrow bandwidth Tm:YAP laser using a pair of etalons," Appl. Opt. **57**, 1468 (2018).
17. C. Jin, D. Li, Y. Bai, Z. Ren and J. Bai, "Wideband tunable graphene-based passively Q-switched Tm:YAP laser," Laser Phys. **25**, 045802 (2015).
18. S. Jackson, "Towards high-power mid-infrared emission from a fibre laser," Nat. Photonics **6**, 423–431 (2012).
19. F. Duarte, *Tunable Lasers Handbook* (Elsevier Science, 1996).
20. J. Jabczynski, L. Gorajek, W. Zendzian, J. Kwiatkowski, H. Jelinkova, J. Sulc and M. Nemec, "High repetition rate, high peak power, diode pumped Tm:YLF laser," Laser Phys. Lett. **6**, 109–112 (2009).
21. B. Yao, L. Ke, X. Duan, G. Li, X. Yang, Y. Ju and Y. Wang, "Stable wavelength, narrow linewidth diode-pumped Tm:YLF laser with double etalons," Laser. Phys. Lett. **6**, 563–566 (2009).
22. A. Korenfeld, D. Sebbag, U. Ben-Ami, E. Shalom, G. Marcus and S. Noach, "High pulse energy passive Q-switching of a diode-pumped Tm:YLF laser by Cr:ZnSe," Laser. Phys. Lett. **12**, 045804 (2015).
23. T. Fan and R. Byer, "Diode laser-pumped solid-state lasers," IEEE Journal of Quantum Electronics **24**, 895–912 (1988).
24. S. Payne, L. Chase, L. Smith, W. Kway and W. Krupke, "Infrared cross-section measurements for crystals doped with Er^{3+}, Tm^{3+} and Ho^{3+}," IEEE Journal of Quantum Electronics **28**, 2619–2630 (1992).

1. Introduction

Lasers operating in the eye-safe 2 μm region have various applications in the fields of medical microsurgery, infrared neural stimulation, plastic material processing, gas spectroscopy, remote sensing, and is well established as a pump source for Ho and Cr doped lasers in the mid IR region [1–7]. Some of those applications require the laser source to have one or more properties such as tunability, narrow spectral bandwidth, nearly diffraction limited beam and pulsed radiation. Notably, there is a growing demand in lasers combining spectral tunability and pulsed operation, allowing more precise control of the laser parameters.

Tm^{3+}-doped lasers are one of the promising radiation sources in the 2 μm region having a broad spectral range emission from the $^3F_4 \rightarrow {}^3H_6$ transition, owing to the relatively sizeable Stark splitting of the low laser energy level $^3H_6$. The exact Stark splitting changes from one host to another, depending on the host matrices symmetry and the effective electric field at the Tm site.

Tunable lasing in Tm-doped materials was widely demonstrated due to the broad gain spectrum of the Tm ions. Works on tunable Tm lasers were reviewed by Godard in [1] up to 2007. Since then, tunability was also achieved in Tm-doped crystals: Tm:$CaYAlO_4$ (1861-2046 nm) [8], Tm:LiLuF (1817-2056 nm) [9], Tm:LuYAG (1935-1995 nm) [10], Tm:LuAG (2018-2029 nm) [11], Tm:LSO (1959-2070 nm) [12, 13], Tm:$LuVO_4$ (1843-1981 nm) [14] and Tm:CLNGG (1896-2069 nm) [15]. Recently, our group reported a tunable narrow bandwidth CW Tm:YAP having a multi-watt level output [16].

Although tunable lasers in this spectral range are very common, only a few of them operate in pulsed mode [12, 13, 17]. Moreover, those above tunable pulsed lasers achieved relative low energy (from 10 up to 180 μJ per pulse). To the best of our knowledge, fiber lasers in this spectral region do not as well demonstrate pulsed tunability at mJ energy level. This is because mJ level pulse energy induces a very high fluence in the small core of the fiber, hence inducing nonlinear effect of four wave mixing and even damage and failure of the gain fiber. Wavelength tuning in pulsed mode is even more difficult. Due to the very high gain in the fiber, the laser tends to emit in the peak wavelength despite the loss introduced by the tuning elements [18].

A number of tuning methods have been developed to control the laser wavelength [3, 19]. These include Volume Bragg Gratings, Lyot filters (LF), Fabry-Perot Etalons, prisms and acousto-optic filters. Despite its limited spectral range, Fabry-Perot Etalon tuning has advantages: simplicity of operation, relatively low cost, as well as operating with a non-polarized beam. Although tuning by LF was implemented in CW Tm:YLF lasers, attempts to obtain a tunable pulsed Tm:YLF were unsuccessful [20], this was mainly due to the low contrast of the LF in the Q-switch regime, where the losses introduced by the LF were insufficient to overcome the high gain accumulated in the crystal.

In addition to the spectral tunability, Fabry-Perot Etalons can also be exploited as bandwidth narrowing components. When using a single Etalon, there is a trade-off between achieving broad free spectral range (FSR) and narrow spectral bandwidth. The use of different thickness Etalons, can maximize both the tuning range and the narrowing effect. Bandwidth narrowing using this method was demonstrated in Tm:YLF only for CW operation [21].

In this paper, we report an actively pulsed tunable narrow bandwidth Tm:YLF laser using a pair of Etalon plates, with mJ level energy pulses. The laser was continuously tuned within a 33 nm wavelength span between 1873 and 1906 nm, having energy pulses ranging from 0.83 to 1.97 mJ. The laser bandwidth was narrowed to ~0.15 nm Full Width at Half Maximum (FWHM) across the whole tunning bandwidth. Tunning and narrowing were also performed in CW operation, having a multi-watt output for all the range from 1873 to 1908 nm. To the best of our knowledge, this is the first time a Tm-doped crystal based laser demonstrates mJ level pulses, with both narrow bandwidth and continuous spectral tunability of 33 nm bandwidth.

2. Experimental setup

The Tm:YLF laser is based on a previous setup used in our lab [22]. The schematic of the Tm:YLF laser is shown in Fig. 1. The pumping arrangement is composed of a 793 nm fiber-coupled laser diode with a 105 μm core diameter, and 0.22 NA. The laser diode can emit up to a maximal power of 19.6 W. The emitted wavelength was temperature tuned to the absorption peak at 793 nm, corresponding to the $^3H_6 \rightarrow {}^3H_4$ transition [2]. The pump beam was delivered and focused in the laser crystal, using a pair of anti-reflection (AR) coated at 650-1050 nm, bi-convex lenses, having 40 and 80 mm focal lengths, respectively. The obtained spot size inside the Tm:YLF crystal was about 250 μm diameter. The Tm:YLF crystal absorbed about 65% of the pump power.

An end-pumped architecture was implemented for the cavity. A plano-plano mirror, having an AR coating at the pump wavelength, and a high reflectance (HR) coating for the 1850-2000 nm was used as a rear cavity mirror. A plano-concave mirror with a 200 mm radius of curvature (ROC) was used as an output coupler (OC). The OC was partially reflecting (PR) coated with 70% reflectance between 1850-2000 nm. The distance between the two mirrors was 200 mm. A 3.5% doped Tm:YLF crystal, 9 mm long and having a 3x3 mm cross-section was used as the gain medium. For this doping concentration, the cross-relaxation process enables to almost double the quantum efficiency of the pumping to the upper laser level. The laser crystal was AR coated at both the pump and laser wavelengths. The crystal was wrapped in indium foil and fastened into an aluminum holder, which was water cooled with a chiller to 18 °C. For the pulsed operation, a water-cooled Acousto-Optic-Modulator (AOM) made of 45 mm long fused silica was used as an

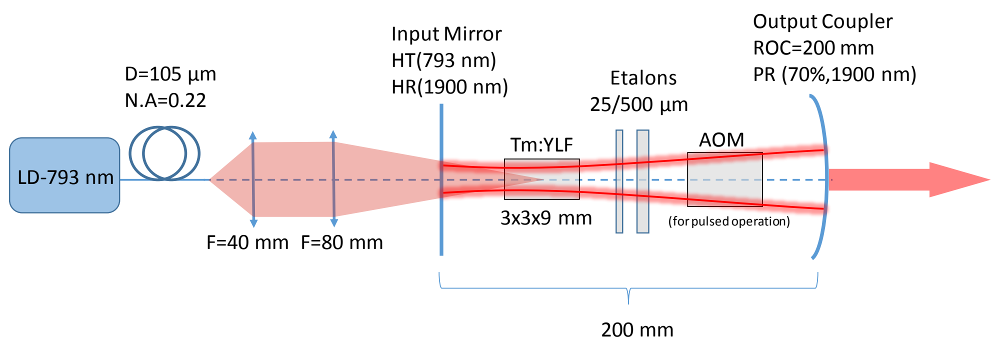

Fig. 1. Schematic of the experimental setup.

active Q-switch and operated at a radio frequency of 68 MHz. Two uncoated Yttrium aluminum garnet (YAG) Etalon plates, with 500 μm and 25 μm thicknesses were fixed on an intracavity rotating stage. The working principle of the Etalon pair will be described further in the discussion section.

The output power was measured, after filtering the residual pump power, using a power meter (Ophir, L50(150)A-35). The laser spectrum was acquired by an OSA (Thorlabs, OSA205C). The pulse energy was measured using an energy meter (Ophir, PE50-C). Pulse temporal characterization was done using 12.5GHz extended InGaAs Photodetectors (EOT, ET-5000) and 100MHz oscilloscope (Agilent, DSO-X 2012A). The M^2 measurement and beam profiling were done using scanning-slit optical beam profiler (Thorlabs, BP209-IR2).

3. Results

The Tm:YLF laser performance for the CW operation without the intra-cavity Etalons, can be seen in Fig. 2(a) as a function of the absorbed pump power. An absorbed pump power at the lasing threshold of 1.9 W was obtained. A maximum output power of 4.57 W was measured at 11.9 W absorbed pump power, corresponding to an optical-to-optical conversion of 38.4%, and a 42.9% slope efficiency obtained from a linear fit of the laser characteristic curve. The optical-to-optical conversion and slope efficiency were calculated relative to the absorbed pump power.

The measured lasing wavelength was 1885 nm, with a spectral width of ~1.4 nm at FWHM. After inserting the Etalon pair inside the laser cavity, the laser achieved a maximum output power of 4.05 W corresponding to an optical-to-optical conversion of 34%, and a 38% slope efficiency at the 1879 nm lasing wavelength Fig. 2(a). The laser wavelength was tuned, in the CW setup, from 1873 to 1908 nm as shown in Fig. 3(a) achieving a continuous tuning range of 35 nm. Along the entire tuning range, the measured output power did not fall below 2.9 W at an absorbed pump power of 11.9 W, as shown in Fig. 3(a). For this narrowed bandwidth tuning operation, a maximum output power of 4.05 W was achieved at a wavelength of 1879 nm.

A 1 kHz repetition rate was chosen, in the active Q-switched mode. The laser average output power for the free-running (without Etalon) pulsed operation is shown in Fig. 2(b). The laser threshold occurred at an absorbed pump power of 3 W. A maximum average output power of 2.25 W was achieved at an absorbed pump power of 8 W, corresponding to an optical-to-optical conversion of 28.1%, and a 44% slope efficiency. The measured emission wavelength was of 1885 nm, and the spectral width was ~1.4 nm FWHM, as shown in Fig. 4. A maximum output

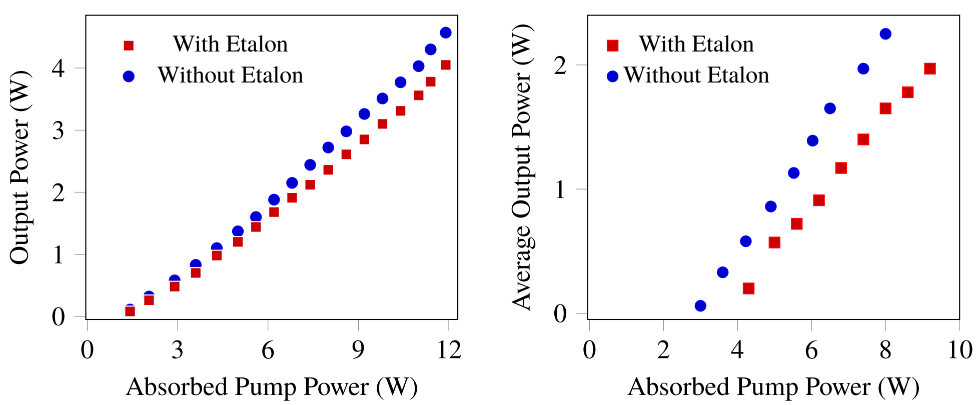

Fig. 2. Tm:YLF output power with and without Etalon plates in CW (left) and pulsed mode (right).

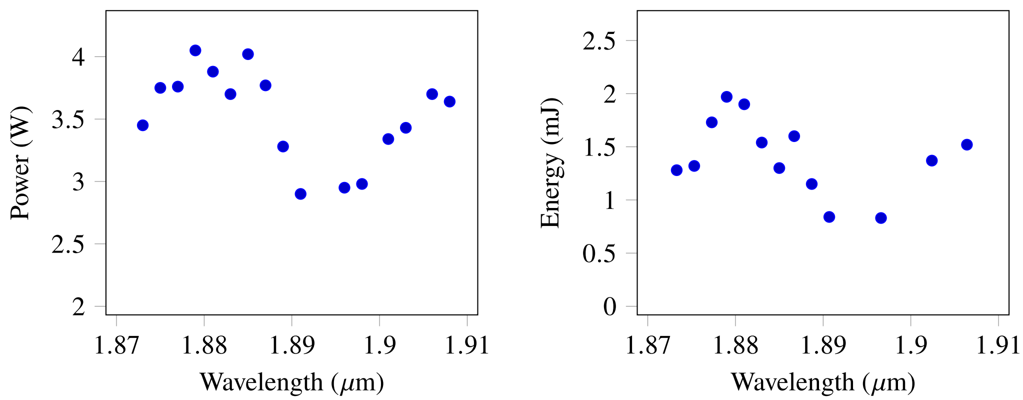

Fig. 3. Tm:YLF spectral tuning in CW (left) and pulsed mode (right).

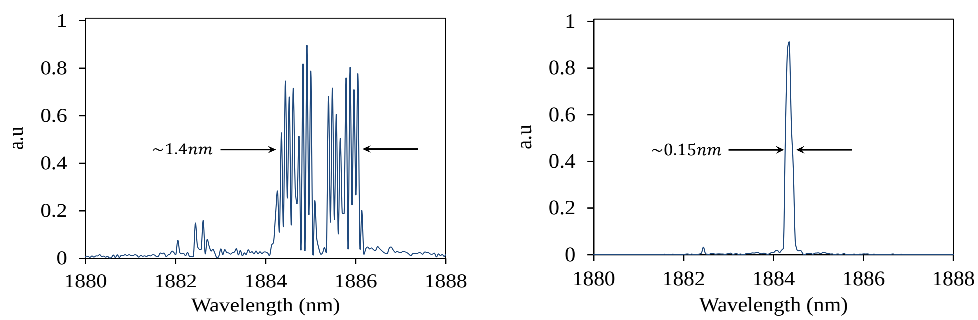

Fig. 4. Tm:YLF spectral width without (left) and with Etalon plates (right).

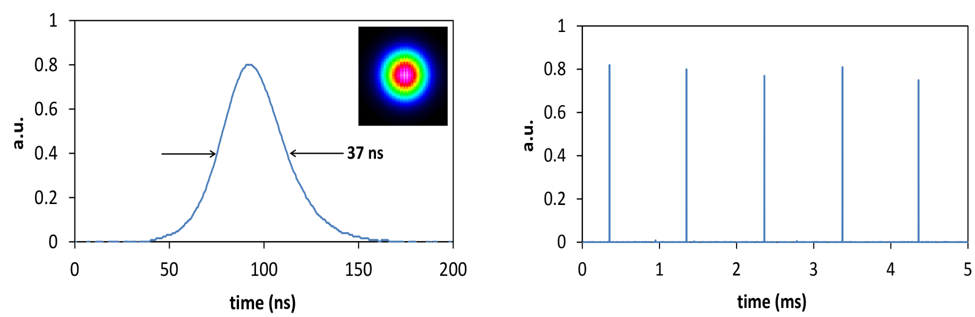

Fig. 5. Tm:YLF pulse duration (left) and pluse train (right). The inset shows the spatial beam profile of the laser with Etalons.

energy of 2.25 mJ was measured, having a pulse duration of 40 ns, corresponding to a peak power of 56.2 kW. After inserting the Etalon pair inside the laser cavity, the laser operated at an absorbed pump power threshold of 3.6 W. A maximum average output power of 1.97 W under an absorbed pump power of 9.2 W was achieved, as shown in Fig. 2(b). The above, corresponding to an energy output of 1.97 mJ, an optical-to-optical conversion of 21.4%, and a 36% slope efficiency. The pulse duration was 37 ns, corresponding to a maximum peak power of 53.2 kW. The temporal characteristics of the pulse duration and pulse train acquired by the oscilloscope are shown in Fig. 5. The laser energy, pulse duration, and peak power in the laser with and

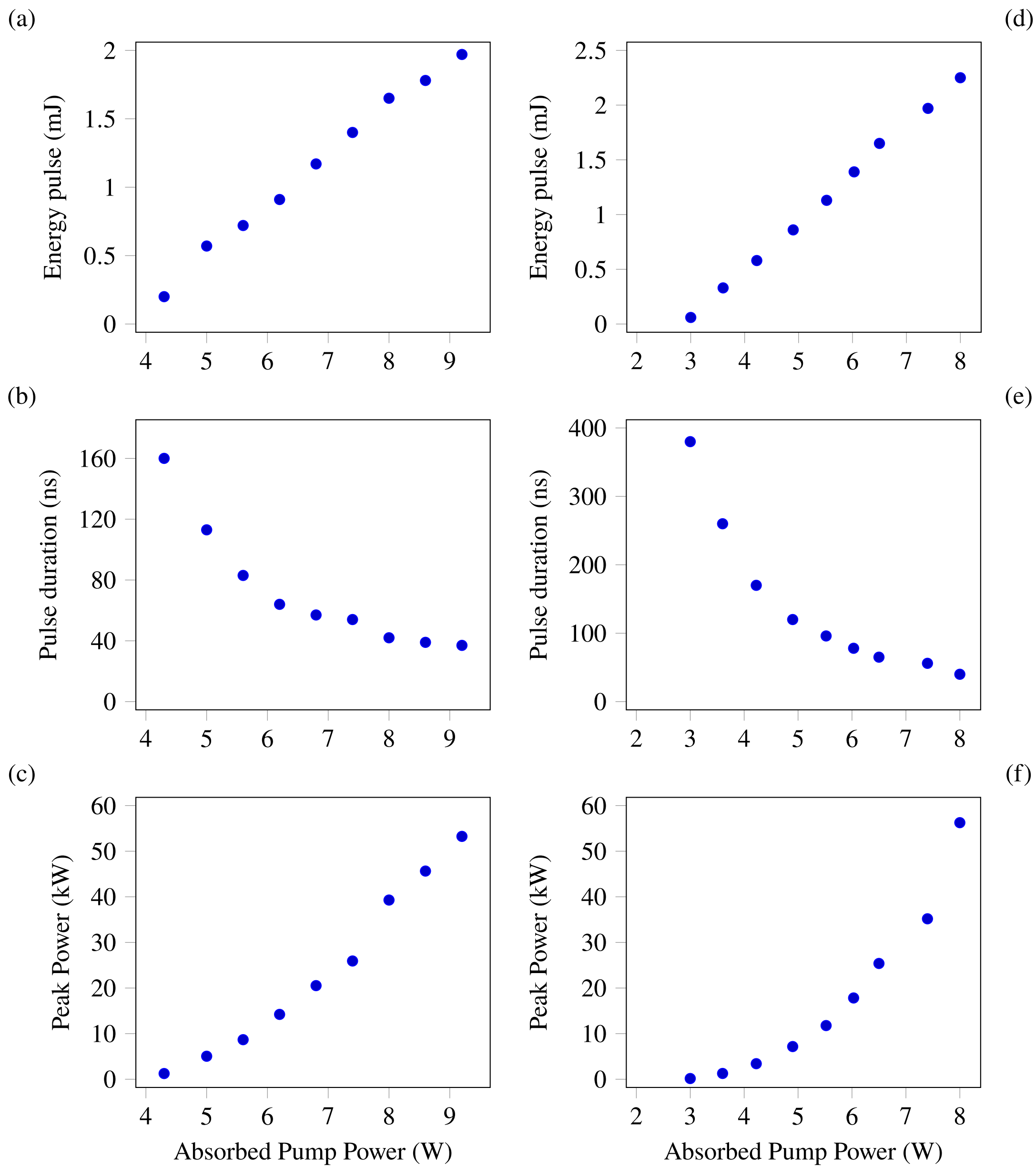

Fig. 6. Laser performances in pulsed mode, with Etalon plates (a,b,c) and without Etalon plates (d,e,f).

without Etalons are shown in Fig. 6. The laser spectral bandwidth was narrowed to ~0.15 nm FWHM, as shown in Fig. 4. This bandwidth was achieved along the whole tunable spectrum, for both the CW and actively Q-switched laser. For all laser configurations, the emission output was completely linearly polarized, having p-polarization up to 1890 nm, and s-polarization for longer wavelengths, match to the polarization dependence of Tm:YLF gain curve.

The laser M^2 was calculated to ~1.2, and the laser spatial beam profile being shown in Fig. 5 (inset to the left). The difference between the laser beam quality M^2 with and without the Etalon

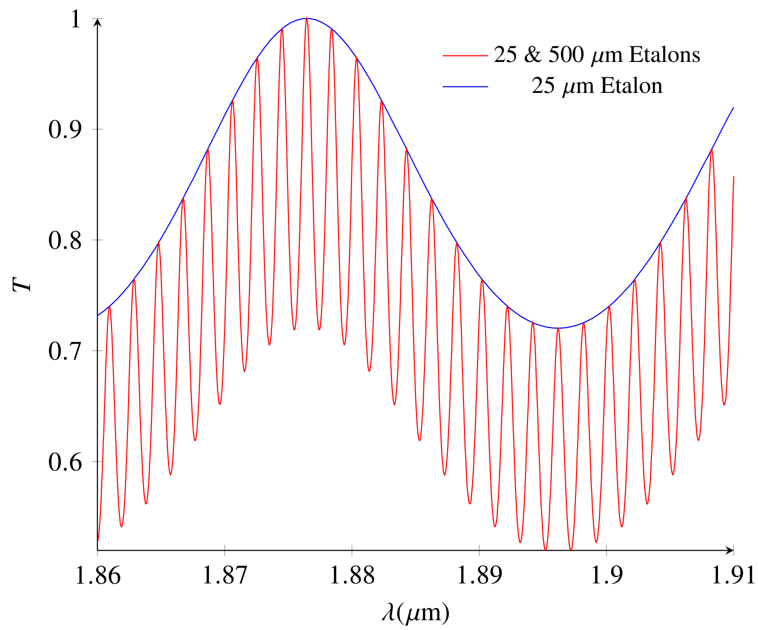

Fig. 7. Free spectral range superposed with two Etalon plates.

plates was relatively negligible.

Compared to the CW operation, the spectral tuning range in the pulsed operation was slightly narrowed, from 35 nm in CW to 33 nm in pulsed mode, and ranged from 1873 to 1906 nm. The tuning range achieved in both cases agrees closely with the 39 nm calculated FSR, of the 25 μm thick Etalon plate, as shown in Fig. 7, This agreement indicates that the measured tuning range was mainly limited by the Etalon pair, and it is suggested that a broader spectral range could be obtained by selecting a thinner Etalon. Along the entire spectral range, the output energy measured did not fall below 0.83 mJ at a constant maximum absorbed pump power of 8.6 W as shown in Fig. 3(b). During the tuning measurements for the pulsed setup, the maximum pump power was reduced to diminish the probability of damaging the laser components.

4. Discussion & conclusion

Following Fan and Byer [23], the threshold for a diode-end-pumped solid state laser can be expressed by:

$$P_{th} \iiint s(r,z) r_p(r,z)\, dV = \frac{\left(\ln\left(\frac{1}{R}\right) + \delta + \ln\left(\frac{1}{T}\right)\right)}{2L\eta} \frac{h\nu_p}{\sigma_{eff}\tau} \tag{1}$$

P_{th} is the threshold pump intensity, s is the normalized laser intensity distribution, and r_p is the normalized pump intensity distribution. Integrating those distributions over the pumped volume yields the beam matching between pump and laser beams. Hence, the left hand side, represent the effective pump intensity at threshold. The right hand side represents the losses of the laser at that point. R is the OC reflectivity, δ is the round-trip losses of the resonator, L is the laser crystal length, η is the pump quantum efficiency, σ_{eff} is the effective stimulated emission cross section, where $\sigma_{eff} = f\sigma$, f is the fraction of the exited electrons used as the upper laser level population, σ is the emission cross section, $h\nu_p$ is the pump photon energy, τ is the upper level fluorescence lifetime.

For quasi-three-level lasers, due to lower laser level population, there is an added term to the losses, which represents the re-absorption mechanism. This population also increases the pump power required to get population inversion. Here, we expand the losses expression, with an added term $\ln(\frac{1}{T})$, appears in formula (1), represents the additional losses taking into account due to the Etalon. T is the transmission of the Etalon given by the Airy formulas:

$$T(\lambda) = \left(1 + \frac{4R_e sin^2(\phi)}{(1 - R_e)^2}\right)^{-1} \quad (2)$$

Here, R_e is the reflectivity of the Etalon surfaces (assuming the same reflectivity from both surfaces), and ϕ quantifies the single-pass phase shift in the Etalon. Regarding the aforementioned experimental setup, each uncoated Etalon surface reflects 8.2% because of Fresnel reflections. The transmission magnitude, varied over the spectrum between 72% to 100% for each of the Etalons. Tilting the Etalon relative the optical axis enables tuning the laser spectrum by selecting a specific wavelength for lasing, corresponding to 100% transmission by the Etalon.

The use of two Etalon plates makes it possible to achieve narrow spectral bandwidth, without reducing the tunability range. The thinner Etalon being responsible for the wide tuning range due to its 39 nm free spectral range (FSR), while the thicker Etalon defines the spectral bandwidth. This principle is demonstrated in Fig. 7, showing the calculated transmission spectrum of this Etalon pair. The transmission spectrum varies inversely to the Etalon's angle, determining which wavelength will have the maximal transmission. By tilting the 25 μm Etalon, it is possible to control the spectral losses. For a tilted Etalon, Fresnel reflections differ from one polarization to another. The Etalon single-pass phase shift ϕ is given by:

$$\phi = \frac{2\pi}{\lambda} n l_e cos(\theta) \quad (3)$$

λ is the light wavelength, n is the refractive index of the Etalon, l_e is the Etalon thickness, and θ is the angle of the Etalon in respect to the optical axis. It is possible, for a given Etalon thickness l_e, to control the wavelength transmission peak by modifying θ.

Maximum transmission occurs when the difference phase shift in the Etalon ϕ is an integer multiple of the wavelength. It is easy to notice that this quantity is independent of R_e. Therefore, the maximum transmission at which there are no added losses due to the Etalon will be regardless of the laser polarization (assuming neglected birefringence), even though, the finesse, and hence the degree of reflectance out of the transmission peak is not the same.

Other tuning methods, make use of tuning devices at Brewster angle forcing polarized emission. This method uses only the p-polarization in the gain curve, hence avoiding participation of the s-polarization to the tuning range. This restriction is in contrast to polarization independent tuning using Etalon.

In the laser presented here, during tuning, the laser output power introduces significant variations as a function of the emitted wavelength. Those power shifts are mainly caused by the wavelength dependent gain spectrum. For the Tm:YLF gain medium, the emission cross section is strongly dependent on wavelength, where there is a significant drop in the gain cross-section, between the 1880 nm and 1908 nm peaks of emission [24]. These slight deviations can be explained by the increase thermal population of the lower laser level for shorter wavelengths, typical to quasi-three-level lasers. Moreover, the emitted polarization of the presented laser strongly depends on the lasing wavelength. The emission up to 1890 nm is p-polarized, while longer wavelengths are s-polarized. These results are with excellent agreement with the reported luminescence of Tm:YLF, as the gain cross-section, is different for the two polarization directions [24].

Despite the output power dependence on the lasing wavelength, the laser configuration demonstrated here allows producing milli-Joule level pulsed lasing across the whole tuning range, limited only by the Etalon pair spectral transmission. Broader tuning range can be expected by optimizing the Etalons parameters.

Optics EXPRESS

In this work, a tunable pulsed Tm:YLF laser was demonstrated, reaching mJ level energy pulses and a tunability range of 33 nm between 1873-1906 nm. The maximum peak power of 53.2 kW is obtained at 1879 nm lasing wavelength. The use of Etalon plates also allowed the laser emission to achieve a narrow bandwidth of ~0.15 nm across the whole tunability range. Narrowing and tunning was also performed in the CW operation, reaching a multi-watt output for all the range from 1873 nm to 1908 nm. The useful combination of high energy pulses with both broad spectral tunability and narrow frequency lasing is presented for the first time, to the best of our knowledge, in a laser based on Tm doped gain media in the 2 μm range. These unique properties significantly enhance the versatility of this kind of laser systems, by allowing the tailoring of both pulse energy and emitted wavelength at the same time, and making this laser a promising tool in the burgeoning 2 μm laser field of applications.

Funding

Israeli Ministry of Science, Technology, and Space (53998)

Acknowledgments

The authors would like to thank Y. Sebbag and Prof. U. Levy from the Hebrew University of Jerusalem for their support, and to R. Nahear for the fruitful discussion and collaboration. This research is supported by the Israeli Ministry of Science, Technology, and Space (53998)